

# Development of a methodology to study the hydrogen embrittlement of steels by means of the small punch test

T.E. García<sup>a,b</sup>, C. Rodríguez<sup>a</sup>, F.J. Belzunce<sup>a</sup>, I. Peñuelas<sup>a</sup>, B. Arroyo<sup>b</sup>

<sup>a</sup> SIMUMECAMAT (University of Oviedo), Edificio Departamental Oeste 7.1.17, Campus Universitario, 33203 Gijón, Spain

<sup>b</sup> LADICIM, Materials Science and Engineering Department, Civil Engineering School, University of Cantabria, Spain

## Abstract

Two different methodologies for analysing the deterioration of mechanical properties due to hydrogen embrittlement by means of the small punch test (SPT) have been studied. In the first, specimens were electrochemically pre-charged before testing, while in the second, they were charged at the same time as testing. A novel, simple, easy-to-manage SPT device was developed for the latter purpose. Two different CrMoV steel grades, a base and a weld metal, tempered at different temperatures, were tested. Tensile tests of hydrogen pre-charged specimens as well as hydrogen content measurements were also performed. Greater hydrogen absorption was observed in the higher strength CrMoV weld metal due to its microstructure composed of low tempered bainite. This steel was fully embrittled in both tensile and small punch tests in the presence of hydrogen, and no significant difference between the two SPT methodologies were found in this case. The CrMoV base metal was only embrittled, however, when hydrogen charging was performed at the same time as testing, showing the greater suitability of this small punch test methodology. The fracture pattern of SPT specimens changed completely from ductile to brittle when testing in hydrogen. Typical SPT parameters also exhibited a marked decrease in ductility and fracture toughness, the CrMoV weld metal being more susceptible to hydrogen embrittlement. Finally, the feasibility of the small punch test for ranking the hydrogen embrittlement susceptibility in steels was demonstrated, and the most suitable SPT parameters for analysing the reduction in mechanical properties were defined.

## 1. Introduction

### 1.1. Background

Hydrogen embrittlement (HE) is a process by means of which the mechanical properties of metals become degraded [1]. Its study is very important in the case of equipment exposed to aggressive environments, such as vessels or pipes employed in the power industry [2–4], off-shore platforms [5] and hydrogen powered vehicles [6,7]. It is also an issue that must be taken into account during manufacturing processes, as hydrogen could be introduced during welding, acid cleaning or in electrolytic coatings [8,9].

The mechanisms which hydrogen employs to damage steels are still relatively unknown. Roughly speaking, they can be divided in three different types of embrittlement [1]:

1. Hydrogen blistering (HB): hydrogen reacts with the surface of the steel, leading to the formation of blisters which act as crack initiators.
2. Environmental hydrogen embrittlement (EHE), which starts with the adsorption of environmental molecular hydrogen by the surface of the steel, followed by absorption within the lattice after dissociation into the atomic form.
3. Internal hydrogen embrittlement (IHE), produced when hydrogen is introduced into the steel in the course of the manufacturing process.

Different methodologies for testing hydrogen embrittlement have been investigated since the publication of the ASTM Selected Technical Paper in 1974 [10]. The most important test applied by industry is the tensile test at low strain rate, the so-called slow strain rate test (SSRT) [2,6,7,11]. However, several researchers have also employed conventional tensile tests with good results [3,12,13]. Both types of test may be performed inside an aggressive environment which provides hydrogen to the steel during testing [6,11], or immediately after pre-charging the specimen with hydrogen [5,7,8,12,13].

The small punch test (SPT) is a quasi-non-destructive test which employs a small amount of material, generally small disks of about 10 mm in diameter and 0.5 mm thick. It was developed in the early 1980s with the aim of estimating the grade of deterioration caused by irradiation in nuclear vessel steels [14,15]. Since then, this miniature test has gained importance due to its capability for estimating (or more properly, ranking) the tensile mechanical [15–17], fracture [15,16,18] or creep properties [19–21] of metallic alloys with high accuracy. A European Code of Practice [22] was developed in 2006, confirming the current importance of the SPT, with several research groups worldwide pushing for its standardization [23].

Several studies have been carried out aimed at estimating hydrogen embrittlement (mainly EHE) deterioration by means of the small punch test [5,24–27]. In a pioneering paper published in 1988, Misawa et al. [24] developed a small punch (SP) testing apparatus using miniaturized specimens submerged in high temperature and high pressure aqueous solutions to assess the resistance to stress corrosion cracking (SCC) and the corrosion of candidate structural steels in water-coolant environment under irradiation. More recently, different researchers have sought to estimate the effect of HE by means of the SPT following two strategies: pre-charging the specimens immediately before testing [5,25], or charging the specimens at the same time as testing [26,27]. The first methodology has the drawback that hydrogen can diffuse out during testing. The main problem with the second methodology is that a special testing device must be used, in some cases employing hydrogen gas at high temperature and pressure, thereby increasing the risk associated with the test.

In order to clarify which SPT methodology might be the most suitable for estimating the deterioration induced by EHE in structural steels, different small punch tests were performed at room temperature, both pre-charging the specimens before testing and charging them at the same time as testing. A novel, simple, easy-to-manage device was developed for the latter purpose. Two different grades of CrMoV steels employed in the petrochemical industry were analysed: a high strength weld metal, which is very susceptible to HE [1,25]; and a base metal usually employed in equipment submitted to hydrogen atmospheres and hence much less susceptible to this phenomenon. Tensile tests with precharged specimens were also conducted in order to compare the results with those obtained by the SPT.

## 1.2. Small punch test parameters and correlations

Fig. 1 shows the characteristic load (P)–punch displacement (d) curve of a ductile metallic alloy, in which different zones have been defined. Zone I corresponds to the elastic bending of the sample along with the indentation produced by the contact of the head of the punch on the surface of the sample. Zone II describes the progressive spread of plastic bending to the entire sample. From a certain moment onward, plastic bending leads to a membrane regime (general plastic deformation), which predominates in most of the curve, this phase corresponding to Zone III. On approaching the maximum load, the slope of the curve decreases due to the failure micromechanisms that arise, resulting in Zone IV, where a visible crack is finally produced and the load decreases until total failure of the specimen occurs.

According to a previous study [16], the SPT load  $P_{y,t/10}$  (calculated at the offset  $t/10$ , where  $t$  is the initial specimen thickness) seems to be the most suitable parameter for estimating the yield strength of structural steels by means of expression (1), where the coefficient  $\alpha$  depends on the material type and testing setup.

$$\sigma_{ys} \approx \frac{P_{y,t=10}}{\alpha \sqrt{t}} \quad \delta 1P$$

$$\sigma_{ut} \approx \frac{\beta_1 P_m}{\sqrt{t}} \quad \delta 2P$$

$$\sigma_{ut} \approx \frac{\beta_2 P_m}{\sqrt{d_m}} \quad \delta 3P$$

$$\epsilon_{qf} \approx \frac{t}{t_f} \ln \frac{t}{t_f} \quad \delta 4P$$

With regard to the estimation of the ultimate tensile strength, both expressions (2) and (3) are found in the literature [15–17,23], expression (2) being the most common ( $P_m$  is the maximum test load and  $d_m$  the displacement at maximum load). Once again, the constants  $\beta_1$  or  $\beta_2$  are dependent on the material and test setup.

On the other hand, some authors have related  $d_m$  with elongation at failure, but the relationships thus obtained are highly dependent on the tested material [16,17]. Nevertheless, it seems to be a good parameter for comparing the ductility of structural steels (the larger the  $d_m$ , the greater the ductility). Another parameter that can be related to the toughness of steel is  $W_m$ , assessed as the area under the SPT curve until the maximum load [25,28,29]. It is also usually used to define the ductile-to-brittle transition temperature.

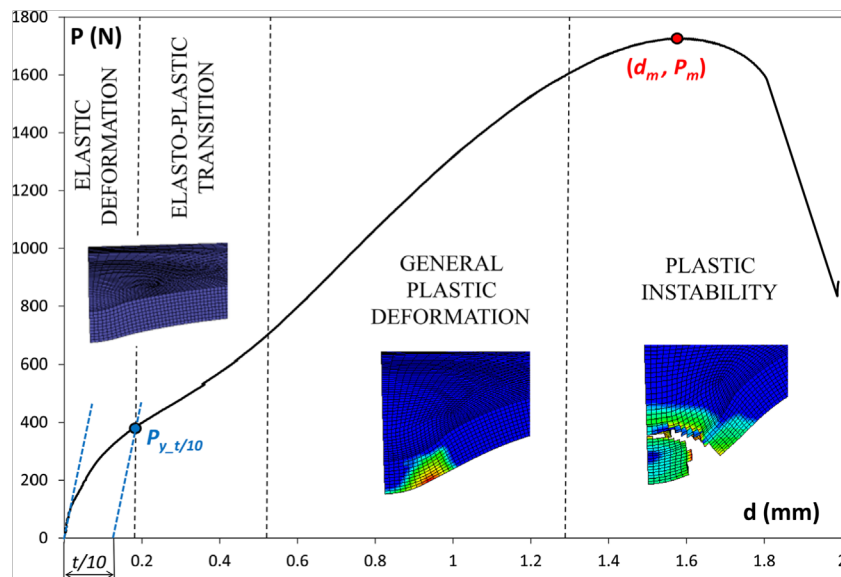


Fig. 1. Typical SPT curve of a structural steel.

Finally, the measurement of the so-called biaxial strain at fracture,  $\epsilon_{qf}$  [15], which relates the original specimen thickness to the minimum thickness measured in the failure zone,  $t_f$  (expression (4)), has also been employed by several authors [15,16,22,31,32] to obtain acceptable predictions of steel fracture toughness. However, very different and fully empirical expressions have been obtained, showing a clear dependence on the type of material.

## 2. Materials and methods

### 2.1. Materials

A 108 mm thick plate of 2.25Cr1Mo0.25V steel (SA 542 Grade D-Class 4) was used as the base metal (CrMoV-1). It was normalized at 950 °C, quenched in water from 925 °C and tempered at 720 °C for 3 h. The chemical composition of this steel is shown in Table 1.

Table 1. Chemical composition of the SA 542 Grade D-Class 4 steel (CrMoV-1) and the weld metal (CrMoV-2) [%wt].

Material	%C	%Si	%Mn	%Cr	%Mo	%V	%Ni
CrMoV-1	0.15	0.09	0.52	2.17	1.06	0.31	0.19
CrMoV-2	0.08	–	–	2.28	0.93	0.24	0.03

A weld coupon with a length of 1300 mm and a width of 600 mm was produced using a maximum gap of 30 mm by means of a submerged arc welding procedure using alternating current, a 4 mm diameter Thyssen Union S1 CrMo2V consumable and a heat input of 2.2 kJ/mm (29–32 V, 425–550 A and 45–55 cm/min). A minimum preheat temperature of 205 °C and a maximum inter-pass temperature of 250 °C were likewise employed. A 4-hour de-hydrogenation treatment was performed at 350 °C immediately after welding. This treatment is absolutely essential at all times when dealing with this steel in order to avoid cold cracking. Table 1 also gives the chemical composition of the weld metal (CrMoV-2).

Fig. 2a shows the microstructure of the CrMoV-1 (base metal), which is composed of tempered martensite. Fig. 2b shows the microstructure of the CrMoV-2 (weld metal), which is composed of fine randomly-oriented acicular bainite packets.

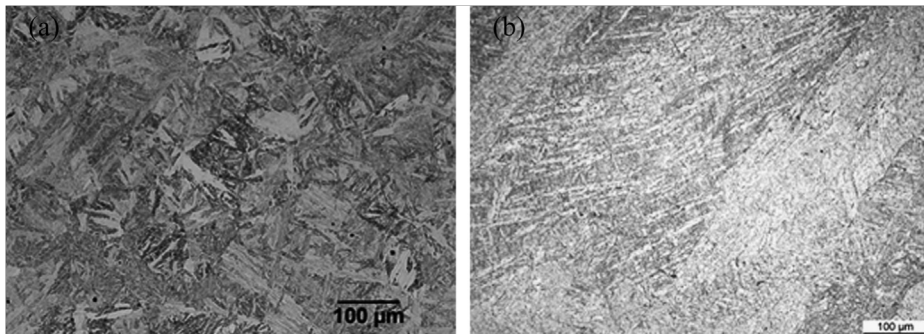


Fig. 2. Microstructures of the CrMoV-1 (a) and CrMoV-2 (b).

### 2.2. Experimental methodology

Fig. 3 shows the geometry and dimensions of both the SPT (Fig. 3a) and plane tensile specimens (Fig. 3b) used in this study. Both types of specimens had the same initial thickness,  $t/0.50070.010$  mm, and were extracted in the directions and positions depicted in Fig. 3c.

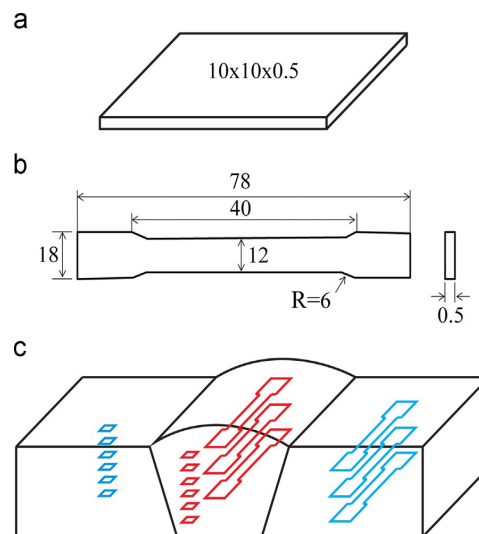


Fig. 3. (a) Dimensions (in mm) of the SPT specimens. (b) Dimensions (in mm) of the tensile specimens. (c) Scheme of the extraction of the specimens from the weld coupon.

Three specimens per steel were electrochemically hydrogen pre-charged at room temperature. A 1 N solution of  $\text{H}_2\text{SO}_4$  in distilled water with 10 drops of  $\text{CS}_2$  and 10 mg of  $\text{As}_2\text{SO}_3$  per litre was employed as electrolyte. The  $\text{As}_2\text{SO}_3$  solution was prepared using the methodology proposed by Pressouyre [33]. Fig. 4a shows one of the devices employed for hydrogen pre-charging both the tensile and the SPT specimens. In the case of tensile specimens, the entire calibrated length was introduced into the electrolyte. In the case of SPT specimens, they were completely submerged in the electrolyte by means of a conductor fastening material, which also allowed several specimens to be submerged at the same time. Two different kinds of electrodes (graphite and stainless steel) were used to supply a  $20 \text{ mA/cm}^2$  current density to the specimen, observing no influence of the type of electrode used. The time of hydrogen charging was 1 h in all cases, as it was experimentally observed that the embrittlement effect stabilised in both types of steels beyond this time. Moreover, it is known that surface damage of the specimens can be produced when using excessively high current densities or charging times during the electro-chemical hydrogen charge [7]. All specimens were mechanically polished (up to 1200 emery paper) and cleaned before hydrogen precharging.

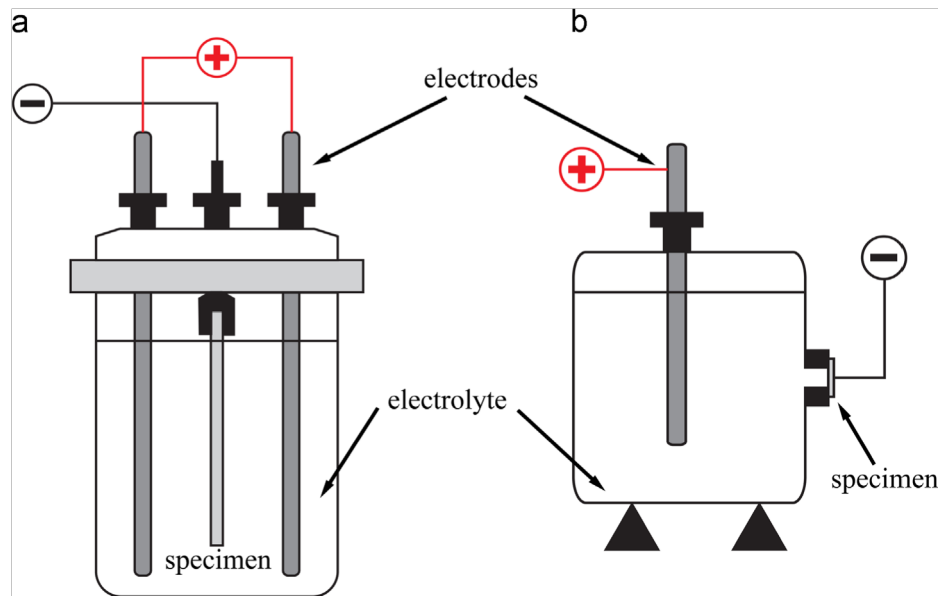


Fig. 4. Devices employed for hydrogen pre-charging: (a) full submersion (b) one-side submersion.

In the case of the SPT specimens, another hydrogen precharging method was also evaluated (Fig. 4b) using a different electrolytic cell. The same electrolyte and current density ( $20 \text{ mA/cm}^2$ ) was employed, the main difference being that only a 4 mm diameter area on one side of the specimen was placed in contact with the electrolyte. The reason for using this latter device was to ascertain whether the degree of embrittlement produced was the same as that obtained after submerging the whole specimen in the electrolyte and thus determine whether a SPT device for charging the specimens during testing, with the electrolyte contacting the specimen only through a 4 mm diameter hole, would be suitable.

Three tensile tests per type of steel (base and weld metal) were performed immediately after extracting the specimens from the electrolytic cell in order to limit hydrogen degassing at room temperature. A universal servo-hydraulic testing machine, equipped with a 15 kN load cell, was employed and the ISO 6892-1:2009 standard [34] was followed. Deformation of the specimens was measured by means of a 4 mm gage length extensometer. Three hydrogen-free specimens were also tested. Mean values of the yield modulus,  $E$ , yield strength ( $0.2\%$  offset),  $\sigma_{\text{yys}}$ , ultimate tensile strength,  $\sigma_{\text{uts}}$ , and elongation at failure,  $e$ , were determined.

Fig. 5a shows a scheme of the small punch test device used to test the hydrogen-free and the pre-charged specimens. A minimum of six specimens of each type (free and pre-charged) was tested. The SPT device was connected to a universal testing machine with a 5 kN load capacity [16,18]. The specimen was placed in the lower matrix, which has a 4 mm diameter hole with a 0.2 mm fillet radius. It was firmly clamped by means of a threaded fixer and the load was applied by means of a 2.5 mm hemispherical diameter punch. A COD-type extensometer was used to accurately measure the punch displacement. A high stiffness material was previously tested in order to measure the machine and equipment stiffness and hence correct the obtained SPT curves [16,30]. All the tests were carried out at a constant displacement rate of 0.2 mm/min employing lubrication to avoid frictional effects. This test setup was in compliance with the SPT Code of Practice [22].

In order to avoid the effect of hydrogen degassing while small punch testing pre-charged specimens and with the aim of simulating a condition closer to the service conditions of real components, tests were also performed in which hydrogen was introduced at the same time as loading. A modified SPT device of similar geometry, but custom designed (Fig. 5b) was employed. The new device had a tank filled with electrolyte placed just above the die hole. A small stainless steel rod, introduced inside this tank, was used as the electrode.

The total hydrogen content of the steels was determined using a Leco DH603 hydrogen analyser based on thermal conductivity measurements after heating the sample above 1100 °C. These determinations were performed on non-charged samples and after hydrogen saturation (pre-charged during 24 h under the aforementioned conditions). In order to avoid hydrogen degassing in these last samples, they were cooled in liquid nitrogen until determining their hydrogen content.

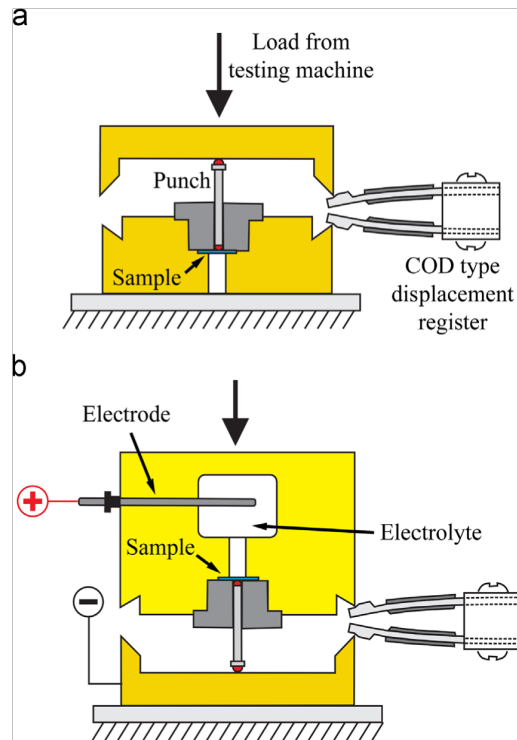


Fig. 5. (a) SPT device for testing hydrogen-free and pre-charged specimens and (b) SPT device for tests performed at the same time as hydrogen charging.

### 3. Results and discussion

Fig. 6 compares the representative true stress ( $\sigma$ )–true strain ( $\epsilon$ ) curves of each steel with those obtained after hydrogen precharging. Table 2 summarizes the average tensile mechanical properties obtained from the two steels and the two analysed conditions. The CrMoV-2 was the only steel embrittled (exhibiting only elastic deformation and final sudden fracture), while no significant differences were observed in the case of the CrMoV-1, demonstrating the lower susceptibility of this steel (quenched and tempered at a high temperature) to hydrogen embrittlement.

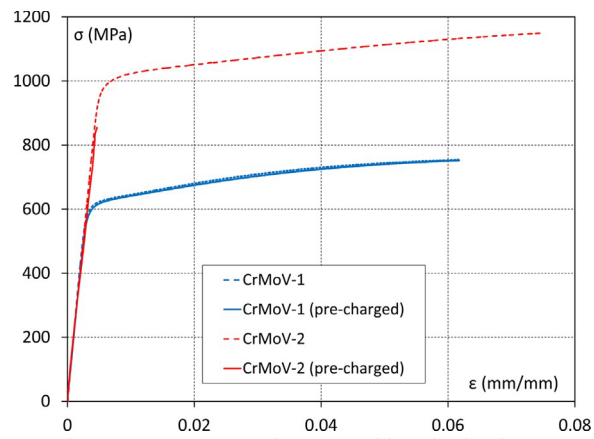


Fig. 6. True stress ( $\sigma$ )–true strain ( $\epsilon$ ) curves of the analysed steels.

Table 2 Average results of tensile tests with hydrogen-free and pre-charged specimens.

CrMoV	Condition	E (GPa)	$\sigma_{ys}$ (MPa)	$\sigma_{ut}$ (MPa)	$\epsilon$ (%)
CrMoV-1	Hydrogen free	201	614	708	20.1
	Hydrogen pre-charged	213	625	716	19.2
CrMoV-2	Hydrogen free	199	993	1067	16.7
	Hydrogen pre-charged	190	851	851	0

Fig. 7 shows the different types of fracture which took place in the CrMoV-2 tensile specimens. In the case of the hydrogen-free samples, a typical ductile fracture along a 45° plane (maximum shear stress) was observed; while in the case of the hydrogen precharged samples, two transversal cracks developed in the lower part of the specimen, indicating that brittle fracture had taken place due to hydrogen pre-charging. Fig. 8 shows SEM micrographs of the tested CrMoV-2 tensile specimens, which highlight the different fracture mechanisms. While ductile mechanisms with nucleation, growth and coalescence of microvoids were predominant in the hydrogen free specimens, a totally brittle mechanism (cleavage) was observed in the hydrogen precharged specimens. Fig. 9 shows representative SPT 'load-displacement' curves of the hydrogen-free CrMoV-2 and the pre-charged specimen using the two methods described previously (full immersion in the electrolyte and one side in contact with it). As can be seen, the behaviour after pre-charging the specimens in the electrolytic cell in Fig. 4a (full immersion of the specimens in the electrolyte) was the same as that obtained with the one-side submerged specimens (Fig. 4b). In fact, one of these latter specimens (CrMoV-2) was tested with the previously submerged surface in contact with the punch (the most stressed surface in this case being the opposite one). The result was very similar, an even lower maximum load being obtained (curve marked with \* in Fig. 9). These results confirmed that hydrogen is able to embrittle the specimen when only a 4 mm diameter area is placed in contact with the electrolyte. This finding has validated the design of the device used for small punch testing at the same time as hydrogen charging (sketched in Fig. 5b).

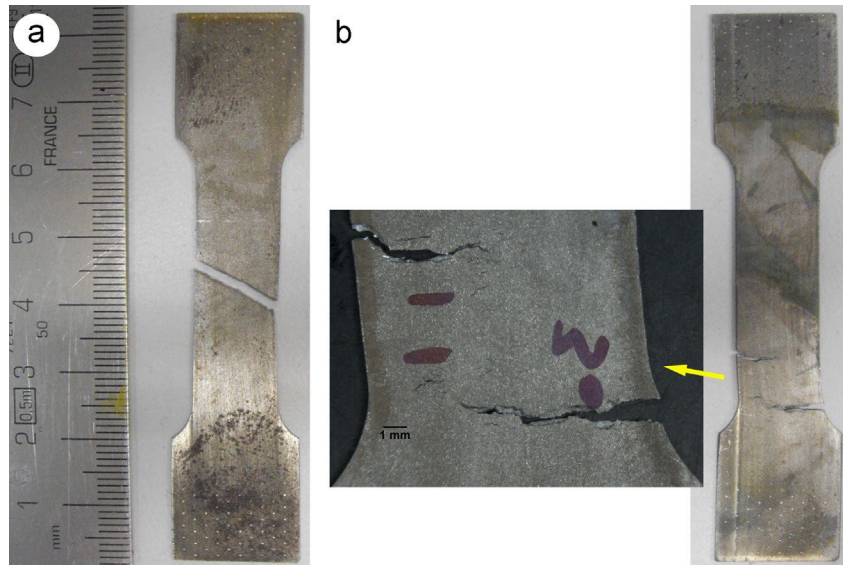


Fig. 7. CrMoV-2 tensile specimens after testing: (a) hydrogen free and (b) hydrogen pre-charged.

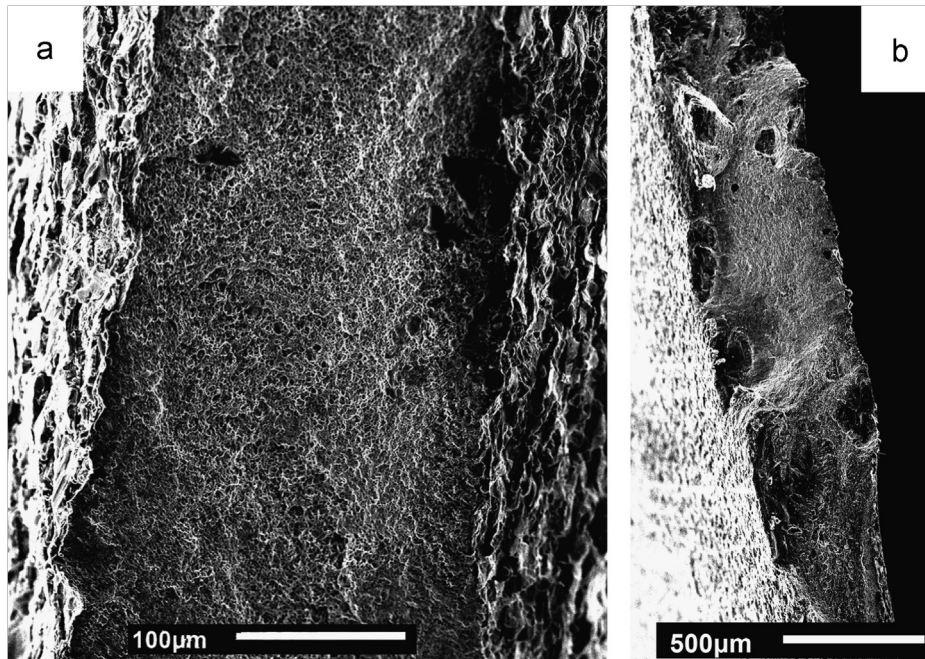


Fig. 8. SEM micrographs of the fracture surfaces of the CrMoV-2 tensile specimens: (a) hydrogen free and (b) hydrogen pre-charged.

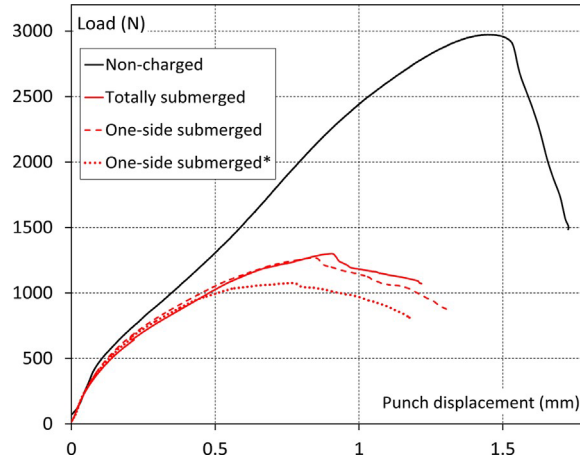


Fig. 9. SPT curves after pre-charging the specimens in different ways (CrMoV-2).

Representative curves obtained with both steels under three different conditions: hydrogen-free, pre-charged in the electrolytic cell and hydrogen charged during mechanical testing, are plotted in Fig. 10. The obtained SPT parameters (mean values/standard deviation) are summarized in Table 3.

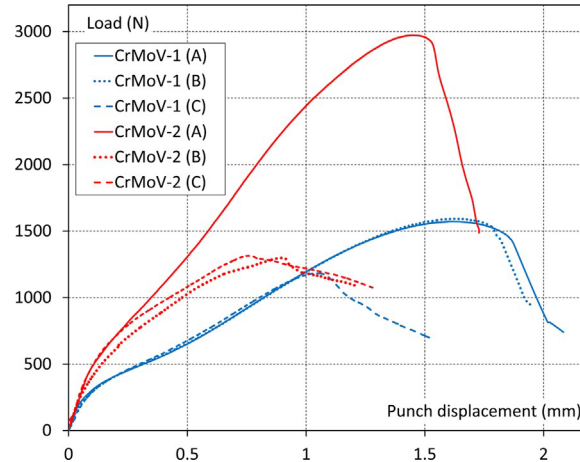


Fig. 10. Representative SPT curves of the steels tested under three different conditions: A – Hydrogen-free; B – hydrogen pre-charged; and C – tested in a hydrogen environment

Table 3. Results of small punch tests (mean/standard deviation) under three different conditions: A – Hydrogen-free; B – hydrogen pre-charged; and C – tested in a hydrogen environment.

CrMoV	Condition	$P_{y\ 1/10/t2}$ (MPa)	$P_m/t^2$ (MPa)	$P_m/(d_m t)$ (MPa)	$d_m$ (mm)	$W_m$ (J)	$\epsilon_{qf}$ (dimensionless)
CrMoV-1	A	14757106	77147623	22317204	1.6270.04	1.6270.10	1.0370.12
	B	1404724	75217103	2089715	1.6370.02	1.5870.05	0.7170.13
	C	1597794	52927549	2413727	1.0270.10	0.7170.14	0.2970.03
CrMoV-2	A	24017146	121387932	37597203	1.5470.05	2.4870.27	0.7070.06
	B	2171794	54637680	32937368	0.8070.16	0.6970.19	0.1670.03
	C	2554782	61257616	36247150	0.8370.06	0.7970.10	0.1870.06

As regards the CrMoV-1, if we compare the SPT results between the hydrogen-free and pre-charged specimens, any important effect of hydrogen pre-charge is detected. Fig. 11 shows a comparison between SEM images of hydrogen-free and pre-charged CrMoV-1 specimens after testing. These specimens exhibited the typical aspect of a ductile fracture in both cases, with a circular crack developing under the punch diameter. A ductile micromechanism (void nucleation, growth and coalescence) can likewise be observed (Figs. 11 b and 11d). No significant differences were found between the SPT parameters of these two conditions, with the exception of  $\epsilon_{qf}$ , which was slightly lower in the case of the pre-charged conditions. Nevertheless, this small decrease was not

considered important, bearing in mind the large scatter in the measurement of this parameter and the fact that no differences were found in the SPT curves or failure pattern.

In contrast, the behaviour of the material in the case of the CrMoV-2 changed drastically between the hydrogen-free and the precharged conditions: while the former behaved in a ductile way, the latter showed mainly brittle failure. The curves for the hydrogencharged product plotted in Fig. 10 have the typical shape obtained when testing brittle materials [16]. Moreover, Fig. 12a shows the fracture aspect of the hydrogen-free specimen, with a circumferential crack where a great amount of microvoids can be observed (Fig. 12b), indicating ductile failure. In spite of this fact, although a circumferential crack was also observed in the hydrogen pre-charged specimen (Fig. 12c), with similar micromechanisms to those observed in Fig. 12b, several radial cracks also developed, denoting brittle behaviour. Transgranular brittle fracture mechanisms were observed in these radial cracks (Fig. 12d). As for the SPT parameters assessed with the pre-charged specimens (Table 3), a decrease was observed when compared with those assessed with the hydrogen-free specimens. Parameters related to ductility and fracture toughness ( $d_m$ ,  $W_m$  and  $\epsilon_{qt}$ ) suffered the largest decrease.

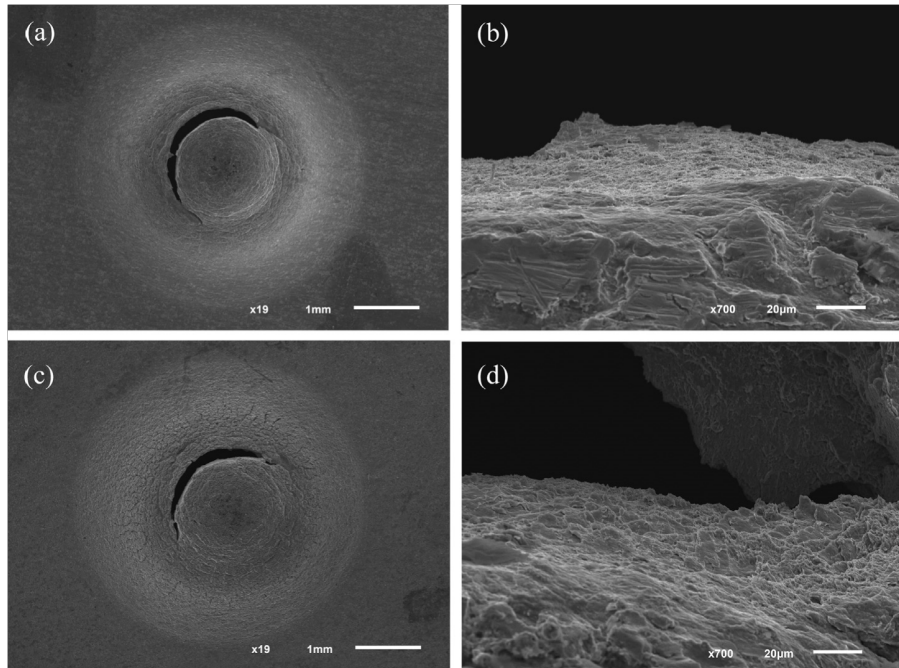


Fig. 11. SEM images of CrMoV-1 specimens: (a) hydrogen-free: general view, (b) hydrogen-free: failed region, (c) hydrogen pre-charged: general view, and (d) hydrogen precharged: failed región

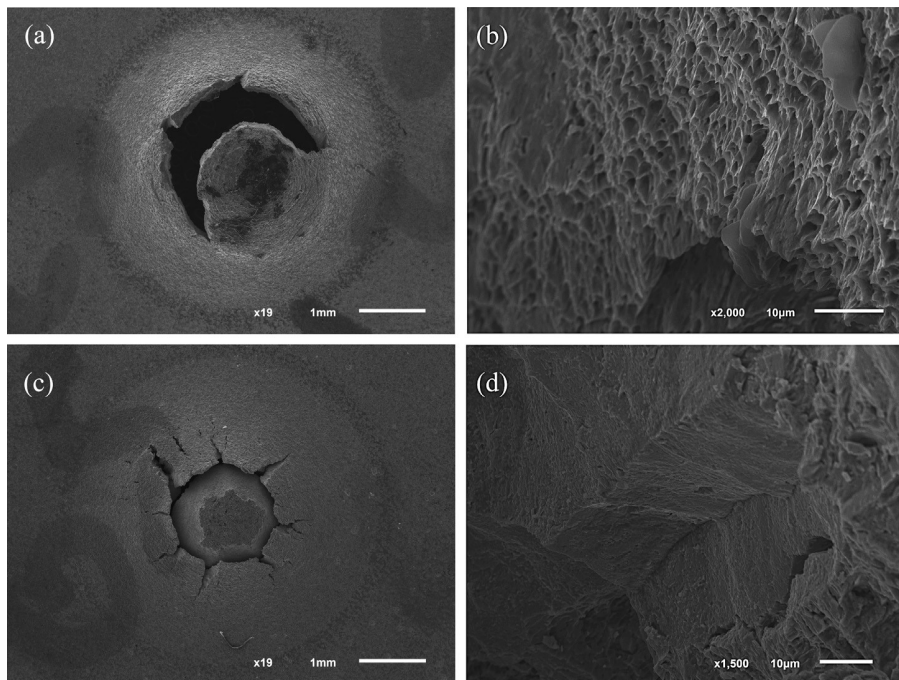


Fig. 12. SEM images of CrMoV-2 specimens: (a) hydrogen-free: general view, (b) hydrogen-free: failed region, (c) hydrogen pre-charged: general view, and (d) hydrogen precharged: failed region, radial crack.

In the case of the SPTs performed at the same time as hydrogen charging, a major change in the SPT behaviour of the CrMoV-1 was observed (Fig. 9 and Table 3). Much lower maximum load and displacement values were obtained, which mainly affected the SPT parameters related to ductility and toughness:  $d_m$ ,  $W_m$  and  $\epsilon_{qf}$ . However, the parameter related with yield strength,  $P_{y,10}/t^2$ , remained practically the same as in the hydrogen-free condition. The shape of the representative SPT curve obtained from this condition, shown in Fig. 10, is now close to that obtained after testing a brittle material. Fig. 13 shows SEM images of one of the tested specimens, which confirm the embrittlement suffered by the steel: numerous radial cracks and crack ramifications were developed. Moreover, not only brittle fracture mechanisms (cleavage and transgranular fracture) were found (see zoom pictures in Fig. 13), but microvoids were also located in the circumferential crack, similar to those shown in Fig. 12b.

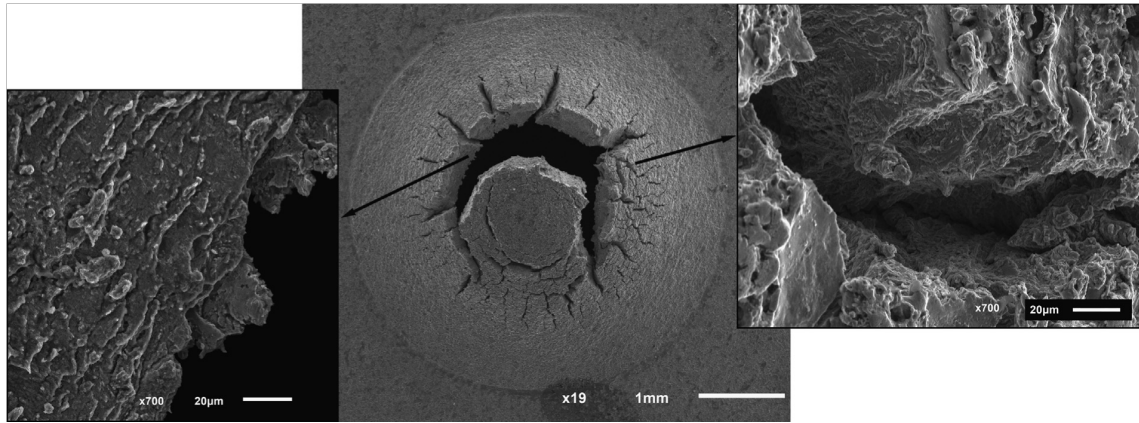


Fig. 13. SEM images of a CrMoV-1 specimen tested at the same time as hydrogen charging.

As regards the CrMoV-2, a very similar level of embrittlement to that obtained after pre-charging the specimen was obtained when the tests were performed at the same time as hydrogen charging, as can be observed by hydrogen-free specimens and SPTs performed at the same time as hydrogen is charged (in fact, it seems to show a small increase in the embrittled condition), indicating that the yield strength of these steels is not very comparing the curves presented in Fig. 10 (SPT curves) and the SPT parameters in Table 3. SEM images of a weld metal specimen tested at the same time as hydrogen charging are shown in Fig. 14. Multiple radial cracks can be observed around a now non-well-defined circumferential crack (Fig. 14a). These cracks were developed by brittle fracture mechanisms, as can be seen in Fig. 14b (transgranular cleavage and intergranular fracture). Some damage at the specimen dome could also be observed (Fig. 14a), denoting greater embrittlement than in the hydrogen pre-charged specimen (compare with Fig. 12c).

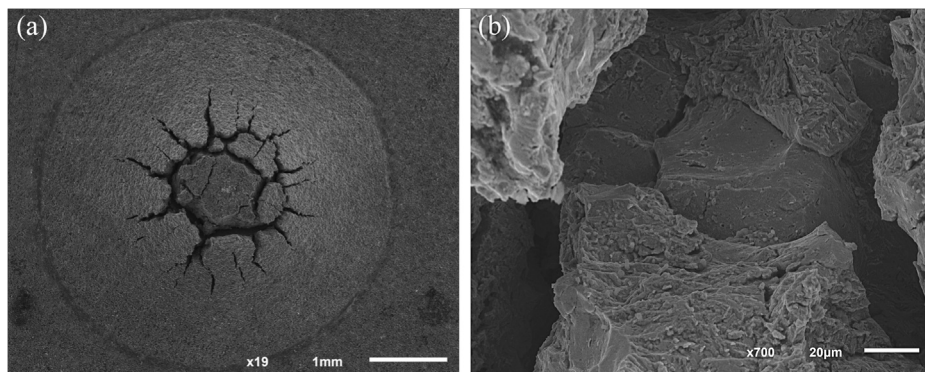


Fig. 14. SEM images of a CrMoV-2 specimen tested in contact with the electrolyte: (a) general view of the failed region and (b) detail of the failed region, radial crack.

Traditionally, the material yield strength is estimated from the SPT by means of expression (1). The criteria for assessing the SPT load,  $P_y$ , can change, but the proposed expression (1) was used because it has shown good results with metallic materials which exhibited both ductile and brittle behaviour [16]. This parameter barely changes between SPTs performed on different under these two conditions. However, the most important observation was the change in mechanical behaviour, from ductile failure in SPT hydrogen-free specimens to brittle failure when hydrogen is charged at the same time as the load is applied. This change can be clearly observed when comparing the SPT curves and the failure pattern of the specimens, which revealed the presence of numerous radial cracks in the embrittled steel instead of a unique circumferential crack in the conventional SPT sample. As for the parameters related to the ultimate tensile strength,  $P_m/t^2$  and  $P_m/(d_{m,t})$ , a marked decrease was observed in the former (31% in case of the CrMoV-1 and 50% in the case of the CrMoV-2), while no significant differences were found in the latter. This finding indicates that the decrease in ultimate tensile strength due to hydrogen embrittlement should be studied by means of the  $P_m/t^2$  parameter. A possible explanation of the poor results obtained with the  $P_m/(d_{m,t})$  parameter is that it only works well with ductile materials [16] and hence is not a suitable parameter when dealing with embrittled materials. The major decrease in the parameters related to ductility and toughness,  $d_m$ ,  $W_m$  and  $\epsilon_{qf}$ , also indicate the drastic change in the mechanical behaviour of the steel. The decrease in the aforementioned parameters was slightly higher in the case of the CrMoV-2. The embrittled specimens of weld metal suffered a 46% decrease in  $d_m$  versus the 37%

decrease in the CrMoV-1. Similarly, there was a 68% reduction in  $W_m$  in the CrMoV-2, while this parameter decreased 56% in the CrMoV-1. The reduction in the parameter related to fracture toughness,  $\epsilon_{qf}$ , was approximately 75% in both steels, although the CrMoV-2 showed more brittle behaviour than the CrMoV-1, with a mean value of 0.18 versus 0.29.

Table 4 shows the results obtained in the hydrogen determination tests. The CrMoV-2 (weld metal) has a somewhat higher hydrogen content than the CrMoV-1 (base metal) in both states, uncharged and after a 24-hour charge (saturation). Microstructural differences between the two steels, low tempered bainite in the case of the CrMoV-2 and high temperature tempered martensite in that of the CrMoV-1, may explain the greater hydrogen absorption observed in the CrMoV-2, which finally also gave rise to a higher susceptibility to embrittlement. The microstructure of the CrMoV-2 with a higher yield strength and greater dislocation density can also explain these differences.

The main goal of this study was not to establish a precise relationship between the SPT parameters and mechanical properties obtained in standard tests. To do so, more steel grades should obviously be tested and standard tensile tests would need to be performed at the same time as hydrogen charging. The main goal of the study was to determine whether the SPT is able to rank the behaviour of structural steels in aggressive hydrogen environments. As was shown, the CrMoV-2 was more susceptible to hydrogen embrittlement than the CrMoV-1, as both tensile tests and the SPT performed on pre-charged specimens showed a marked decrease in mechanical properties and in the characteristic SPT parameters in the case of the former steel. The CrMoV-1 exhibited a higher resistance to hydrogen embrittlement, as no significant difference was observed with hydrogen-free and hydrogen pre-charged tensile and SPT specimens. The CrMoV-2 has a very similar chemical composition to the base steel CrMoV-1, but quite a different microstructure, bainite tempered at only 350 °C (de-hydrogenation treatment) instead of high temperature (720 °C) tempered martensite, and a much greater yield strength and ultimate tensile strength. It is well known that hydrogen embrittlement increases with increasing steel yield strength [3,4,6].

Table 4. Hydrogen content (in ppm) of both uncharged and 24- h charged steels (mean  $\pm$  standard deviation).

CrMoV	Uncharged	24 h
CrMoV-1	1.070.1	10.672.3
CrMoV-2	1.670.5	13.671.5

It should also be noted that, when dealing with the CrMoV-1 steel, it was necessary to perform the SPT at the same time as charging in order to promote hydrogen embrittlement. Under the aforementioned condition, embrittlement was fully achieved, as hydrogen had been continuously introduced in the most stressed region of the specimen (convex side), facilitating the diffusion of larger quantities of hydrogen to the process zone where the greatest plastic deformation takes place and fracture mechanisms initiate. As in many real situations, in which mechanical loading takes place at the same time as hydrogen enters the material, the SPT methodology, in which hydrogen charging takes place at the same time as testing the specimens, is more suitable to study the effect of hydrogen and to rank the behaviour of different materials. However, when hydrogen pre-charged specimens are used, only steels which are severely embrittled by hydrogen, such as the CrMoV-2, are mechanically affected.

All the aforementioned findings show that the small punch test can be a powerful tool for ranking the resistance of materials to environmental hydrogen embrittlement (EHE), especially if the specimen is hydrogen charged at the same time as testing. Many advantages of this latter methodology may be highlighted. First of all, SP tests only require a small piece of material, and very small regions of structural components (such as the heat affected zones of welded joints or surface treated regions) can be tested. The small size of the SPT device also allows working with small volumes of electrolyte (in the order of ml), which is very convenient to improve safety conditions in the laboratory. Another very important aspect is that the low thickness of the SPT specimens (0.5 mm) means that room temperature hydrogen charging only requires a short time to take place.

#### 4. Conclusions

The following conclusions can be drawn from the present study:

- The feasibility of the small punch test for ranking hydrogen embrittlement in steels was demonstrated.
- Small punch test specimens can be effectively hydrogen embrittled by passing the selected current density onto a small area of the sample in contact with the electrolyte.
- A more embrittled condition is obtained when the SPT specimen is hydrogen charged at the same time as testing, as this methodology was shown to be able to embrittle steels that were not embrittled when the SPT was performed after hydrogen pre-charging.
- The SPT  $P_m/t^2$  parameter is the most suitable SPT parameter for analysing the reduction in strength properties in the case of hydrogen embrittled steels.
- The SPT parameters  $d_m$  and  $W_m$  seem to be suitable for analysing the decrease in ductility and toughness which takes place in hydrogen embrittled structural steels. The biaxial strain at fracture,  $\epsilon_{qf}$ , can also be used for estimating the reduction in fracture toughness of hydrogen embrittled steels.
- The CrMoV-2 (weld metal) is more susceptible to hydrogen embrittlement than the CrMoV-1 (base metal) due to the higher yield strength and ultimate tensile strength of the former, mainly as a result of the application of a lower temperature tempering treatment.

## Acknowledgements

The authors gratefully acknowledge funding from the Ministry of Science and Innovation of Spain through project MICINN-12MAT2011-28796-C03-03. T.E. García also acknowledges financial support from the Principado de Asturias Government through the Severo Ochoa Programme (BP12-160).

## References

- [1] G.P. Tiwari, A. Bose, J.K. Chakravarty, et al., *Mater. Sci. Eng. A—Struct.* **A286** (2000) 269–281.
- [2] A.H.S. Bueno, E.D. Moreira, J.A.C.P. Gomes, *Eng. Fail. Anal.* **36** (2014) 423–431. [3] R.A. Siddiqui, H.A. Abdullah, *J. Mater. Process Technol.* **170** (2005) 430–435.
- [4] R.K. Dayal, N. Parvathavarthini, *Sadhana—Acad. Proc. Eng. Sci.* **28** (2003) 431–451.
- [5] B. Arroyo, J.A. Álvarez, R. Lacalle, F. Gutiérrez-Solana, T.E. García, Environmental effects on R5 steel under cathodic protection and cathodic charge. Characterization using the small punch tests, in: *Proceedings of the 3rd International Conference SSTT, Graz, Austria, 2014.*
- [6] T. Michler, J. Naumann, *Int. J. Hydrog. Energy* **35** (2010) 1485–1492.
- [7] J. Rehr, K. Mraczek, A. Pichler, E. Werner, *Mater. Sci. Eng. A—Struct.* **590** (2014) 360–367.
- [8] V.I. Shvachko, *Int. J. Hydrog. Energy* **25** (2000) 473–480.
- [9] G. Magudeeswaran, V. Balasubramanian, G.M. Reddy, *Int. J. Hydrog. Energy* **33** (2008) 1897–1908.
- [10] H.H. Gray, *ASTM STP* **543**, 1974, p. 3.
- [11] H. Xu, X. Xia, L. Hua, Y. Sun, Y. Dai, *Eng. Fail. Anal.* **19** (2012) 43–50.
- [12] Y. Yagodinskyy, E. Malitckii, M. Ganchenkova, et al., *J. Nucl. Mater.* **444** (2014) 435–440.
- [13] Y. Wang, X. Wang, J. Gong, L. Shen, W. Dong, *Int. J. Hydrog. Energy* **39** (2014) 1309–13918.
- [14] M.P. Manahan, A.S. Argon, O.K. Harling, *J. Nucl. Mater.* **104** (1981) 1545–1550. [15] X. Mao, H. Takahashi, *J. Nucl. Mater.* **150** (1987) 42–52.
- [16] T.E. García, C. Rodríguez, F.J. Belzunce, C. Suárez, *J. Alloys Compd.* **582** (2014) 708–717.
- [17] E. Fleury, J.S. Ha, *Int. J. Press. Vessel Pip.* **75** (1998) 699–706.
- [18] T.E. García, C. Rodríguez, F.J. Belzunce, I.I. Cuesta, Fracture toughness estimation of structural steels by means of the CTOD measured in notched small punch specimens, in: *Proceedings of the 3rd International Conference SSTT, Graz, Austria, 2014.*
- [19] P. Dymáček, K. Milicka, *Mater. Sci. Eng. A—Struct.* **510–511** (2009) 444–449. [20] M.T. Whittaker, W.J. Harrison, R.J. Lancaster, S. Williams, *Mater. Sci. Eng. A—Struct.* **577** (2013) 114–119.
- [21] M. Lorenzo, I.I. Cuesta, J.M. Alegre, *Mater. Sci. Eng. A—Struct.* **614** (2014) 319–325.
- [22] CEN Workshop Agreement, CWA 15627:2006 E, Small Punch Test Method for Metallic Materials, CEN, Brussels, 2006.
- [23] R. Hurst, K. Matocha, Experiences with the European Code of Practice for small punch testing for creep, tensile and fracture behaviour, in: *Proceedings of the 3rd International Conference SSTT, Graz, Austria, 2014.*
- [24] T. Misawa, Y. Hamaguchi, M. Saito, *J. Nucl. Mater.* **155–157** (1988) 749–753.
- [25] S.-I. Komazaki, A. Koyama, T. Misawa, *Mater. Trans.* **43–49** (2002) 2213–2218.
- [26] T. Nambu, K. Shimizu, Y. Matsumoto, et al., *J. Alloy. Compd.* **446–447** (2007) 588–592.
- [27] Y. Matsumoto, H. Yukawa, T. Nambu, Quantitative evaluation of hydrogen embrittlement of metal membrane detected by in-situ small punch test under hydrogen permeation, in: *Proceedings of the 1st International Conference SSTT, Ostrava, Czech Republic, 2010.*
- [28] N. Okuda, R. Kasada, A. Kimura, *J. Nucl. Mater.* **386–388** (2009) 974–978.
- [29] C. Rodríguez, J. García, E. Cárdenas, F.J. Belzunce, C. Betegón, *Weld. J.* **88** (2009) 188–192.
- [30] E.N. Campitelli, P. Spätig, R. Bonadé, W. Hoffelner, M. Victoria, *J. Nucl. Mater.* **335** (2004) 366–378.
- [31] E. Budzakoska, D.G. Carr, P.A. Stathers, et al., *Fatigue Fract. Eng. M* **30** (2007) 796–807.
- [32] K. Guan, L. Hua, Q. Wang, et al., *Nucl. Eng. Des.* **241** (2011) 1407–1413.
- [33] G.M. Pressouyre, Role of trapping on hydrogen transport and embrittlement. Ph.D. thesis, Carnegie Mellon University, 1977.
- [34] ISO 6892-1:2009, Metallic materials – Tensile testing – Part 1: Method of Test at Room Temperature, ISO European Standards